JPET Fast Forward. Published on March 23, 2011 as DOI: 10.1124/jpet.111.179390

Increased Activation of Wnt/β-catenin Pathway in Spontaneous Hepatocellular Carcinoma observed in Farnesoid X Receptor Knockout Mice.

Andy Wolfe, Ann Thomas, Genea Edwards, Reshma Jaseja, Grace L. Guo and Udayan Apte

Department of Pharmacology, Toxicology and Therapeutics, University of Kansas Medical Center, Kansas City, KS. AW, AT, GE, RJ, GLG, UA

JPET Fast Forward. Published on March 23, 2011 as DOI: 10.1124/jpet.111.179390
This article has not been copyedited and formatted. The final version may differ from this version.

Running Title: Role of β-catenin in hepatocellular carcinoma in FXR-KO mice

Corresponding Author:

Udayan Apte, PhD, DABT

Department of Pharmacology, Toxicology and Therapeutics,

University of Kansas Medical Center,

KLSIC 4087-MS1018,

3901 Rainbow Blvd, Kansas City, KS 66160.

Tel: 913-588-9247

Fax: 913-588-7501

E-mail: uapte@kumc.edu

Number of text pages: 35

Number of tables: 2 (1 in text and 1 supplemental)

Number of figures: 7 (+1 supplemental)

Number of references: 47

Number of words in the Abstract: 250

Number of words in the Introduction: 419

Number of words in the Discussion: 1285

Abbreviations: FXR, Farnesoid X Receptor; HCC, Hepatocellular Carcinoma; GSK-3β, glycogen synthase kinase 3β; Dishevelled, Dvl; Frizzled, Fzl

Recommended section: Gastrointestinal, Hepatic, Pulmonary, and Renal

JPET Fast Forward. Published on March 23, 2011 as DOI: 10.1124/jpet.111.179390
This article has not been copyedited and formatted. The final version may differ from this version.

Abstract

Farnesoid X Receptor (FXR), the primary bile acid sensing nuclear receptor is also known for its anti-cancer properties. It is known that FXR deficiency in mice (FRX-KO) results in spontaneous hepatocellular carcinoma (HCC) but the mechanisms are not completely understood. Here we report that sustained activation of Wnt/β-catenin pathway is associated with spontaneous HCC in FXR-KO mice. HCC development was studied in FXR-KO mice at 3, 8 and 14 months of age. No tumors were observed at either 3 or 8 months but presence of HCC was observed in 100% of the FXR-KO mice at the age of 14 months. Further analysis revealed no change in β-catenin activation in the livers of 3-month-old FXR-KO mice but a moderate increase was observed in 8-month-old FXR-KO mice. β-Catenin activation further increased significantly in 14-month-old tumor bearing mice. Further analysis revealed two independent mechanisms might be involved in β-catenin activation in the FXR-KO livers. Activation of canonical Wnt signaling was evident as indicated by increased Wnt4 and dishevelled (Dvl) expression along with GSK-3β inactivation. We also observed decreased expression of E-cadherin, a known regulator of β-catenin, in FXR-KO mice. The decrease in E-cadherin expression was accompanied by increased expression of its transcriptional repressor, Snail. Consistent with the increased HCC in FXR-KO mice we observed significant decrease in FXR expression and activity in human HCC samples. Taken together, these data indicate that temporal increase in activation of Wnt/β-catenin is observed during spontaneous HCC development in FXR-KO mice and is potentially critical for tumor development.

JPET Fast Forward. Published on March 23, 2011 as DOI: 10.1124/jpet.111.179390
This article has not been copyedited and formatted. The final version may differ from this version.

Introduction

Farnesoid X Receptor (FXR) is the main bile acids-sensing receptor in the body expressed in high levels in the liver and the gut (Forman et al., 1995; Sinal et al., 2000; Wang et al., 2008). Role of FXR has been recognized in a variety of physiological and pathological processes including regulation of bile acid homeostasis (Guo et al., 2003; Lambert et al., 2003; Eloranta and Kullak-Ublick, 2008; Gadaleta et al., 2010), lipid metabolism, liver regeneration, inflammation and cancer (Huang et al., 2006; Modica et al., 2008; Wang et al., 2008). It is known that loss of FXR as observed in the whole body FXR knockout (FXR-KO) mice results in increased carcinogenesis of the colon and the liver (Kim et al., 2007b; Yang et al., 2007; Maran et al., 2009). FXR-KO mice develop spontaneous hepatocellular carcinoma (HCC) at the age of 12-14 months but the mechanisms remain unknown (Kim et al., 2007b; Yang et al., 2007). It is known that FXR-KO mice have 4-fold higher total bile acids and decrease in bile acids using cholestyramine has been shown to decrease HCC incidence in the FXR-KO mice (Yang et al., 2007). However, the exact role of FXR or subsequent increase in bile acids in pathogenesis of HCC is not known.

Wnt/β-catenin pathway plays a central role in liver biology and is involved in embryonic and postnatal liver development, liver regeneration, hepatic progenitor cell biology and pathogenesis of liver cancer (Monga and Michalopoulos, 2005; Thompson and Monga, 2007). Mutations in *CTNNB1*, the gene that encodes β-catenin protein, the downstream effector of the Wnt/β-catenin pathway, are observed in a large portion of HCC. Furthermore, increased β-catenin activation is observed in majority of HCC (Carruba et al., 1999; Huang et al., 1999; Devereux et al., 2001; Fujie et al., 2001;

JPET Fast Forward. Published on March 23, 2011 as DOI: 10.1124/jpet.111.179390
This article has not been copyedited and formatted. The final version may differ from this version.

Calvisi et al., 2004a). A substantial increase in activation of β-catenin has also been observed in hepatoblastomas, the primary hepatic malignancy in children (Taniguchi et al., 2002; Monga et al., 2003). Furthermore, increased expression in Wnt proteins, the extracellular ligands of the Wnt/β-catenin pathway, and decrease in expression of Dickkopf-1 (DKK-1) and soluble frizzled related protein (sFRP), the inhibitors of Wnt signaling, have been observed in various cancers (Kolligs et al., 2002).

We hypothesized that spontaneous hepatocarcinogenesis in FXR-KO mice is associated with β-catenin activation. We investigated activation of Wnt/β-catenin pathway during tumorigenesis in the FXR-KO mice over a time course of 3 to 14 months. Our studies demonstrate sustained activation of β-catenin and reveal the mechanisms behind increased β-catenin activation in FXR-KO livers.

JPET Fast Forward. Published on March 23, 2011 as DOI: 10.1124/jpet.111.179390
This article has not been copyedited and formatted. The final version may differ from this version.

Material and Methods

Antibodies.

The primary antibodies used in these studies were as follows: mouse anti-β-catenin (BD Biosciences), mouse anti-activated β-catenin (Millipore), rabbit anti-GSK-3β, rabbit anti-Ser9-Phospho-GSK-3β, rabbit anti-Ser45-Thr41-phospho-β-catenin, rabbit anti-E-cadherin, rabbit anti-Snail, and rabbit anti-dishevelled (Cell Signaling Technologies, Danvers, MA), Wnt4 (Santa Cruz Biotech, Santa Cruz, CA). All Western blotting secondary antibodies were purchased from Cell Signaling Technologies and biotinylated secondary antibodies for immunohistochemistry were purchased from Jackson Immunoresearch (West Grove, PA).

Animals and Tissue Harvesting.

Three month old (n=5), 8 month old (n=5), 12-14 month old FXR-KO (n=17) and WT (C57BL/6, n=10) mice were used in these studies. FXR-KO mice used in these studies are backcrossed into the C57BL/6 genetic background for 10 generations and have been described in detail previously (Maran et al., 2009). All animals were housed in Association for Assessment and Accreditation of Laboratory Animal Care-accredited facilities at the University of Kansas Medical Center under a standard 12-h light/dark cycle with access to chow and water *ad libitum*. The Institutional Animal Care and Use Committee approved all studies. Mice were killed by cervical dislocation under isofluorane anesthesia and livers were collected. Pieces of liver were fixed in 10% neutral buffered formalin for 48 h, further processed to obtain paraffin blocks and 4μm thick sections were obtained. A piece of liver was frozen in OCT and used to obtain

fresh frozen sections. A part of liver tissue was used to prepare fresh nuclear and cytoplasmic protein extracts using the NE-PER Nuclear and Cytoplasmic Extraction Reagents (Pierce, Rockford, IL). The remaining liver tissue was frozen in liquid N_2, and stored at -80^{0}C until used to prepare RIPA extracts.

Protein isolation and Western Blotting.

Total protein was isolated from WT and FXR-KO livers using in RIPA buffer (1% SDS, 20 mM Tris/Cl pH 7.5, 150 mM NaCl, 0.5% NP-40, 1% Triton X-100, 0.25% Sodium Deoxycholate). Protease and Phosphatase inhibitors (Halt Protease and Phosphatase Inhibitor Cocktail with EDTA, Pierce, Rockland, IL, catalog# 78446) at a concentration of 1:100 were freshly added to the RIPA buffer before use. Cell lysates were prepared using glass homogenizers. Protein concentrations of all lysates were determined using the bicinchoninic acid protein assay reagents (BCA method) (Pierce, Rockford, IL). Total cell lysates made in RIPA buffer (50 µg) were separated by electrophoresis on 4% to 12% NuPage Bis-Tris gels with MOPS buffer (Invitrogen, Carlsbad, CA), then transferred to Immobilon-P membranes (Millipore, Bedford, MA) in NuPAGE transfer buffer containing 20% methanol. Membranes were stained with Ponceau S to verify loading and transfer efficiency. Membranes were probed with primary and secondary antibodies in Tris-buffered saline with Tween-20 (TBS-T) containing either 5% nonfat milk or 5% bovine serum albumin depending on the antibody used. Signal was visualized by incubating the blots in SuperSignal West Pico chemiluminescence substrate (Pierce, Rockford, IL) and exposing to X-ray film (MidSci, St. Louis, MO).

Immunohistochemistry and Immunofluorescence.

JPET Fast Forward. Published on March 23, 2011 as DOI: 10.1124/jpet.111.179390
This article has not been copyedited and formatted. The final version may differ from this version.

Paraffin-embedded liver sections (4 μm thick) were used for immunohistochemical staining. Antigen retrieval was achieved by the citrate buffer method. Slides were placed in boiling citrate buffer solution for 5 min followed by 10 min at sub-boiling temperature. The tissue sections were blocked in either 5% normal goat serum for 30 minutes or the Ultra V Block solution (Thermo Scientific, Fremont, CA) for 5 minutes followed by incubation with pertinent primary antibody overnight at 4°C. The primary antibody was then linked to biotinylated secondary antibody followed by routine avidin-biotin complex method (ABC Vectastain kit, Vector Laboratories, Burlingame, CA). Diaminobenzidine was used as the chromogen, which resulted in a brown reaction product. Immunofluorescence staining of β-catenin was performed using fresh frozen sections as described previously (Monga et al., 2006).

Real Time PCR.

To quantify Wnt and Fzl mRNA levels, TaqMan-based Real Time PCR arrays (Applied Biosystems, Carlsbad, CA) were used. Total RNA was isolated from 8 and 14 month old WT and FXR-KO livers using Trizol method according to Manufacturer's protocol (Sigma, St. Louis, MO) and converted to cDNA as previously described (Apte et al., 2009). Real Time PCR was performed on StepOnePlus Real time PCR machine (Applied Biosystems, Carlsbad, CA). The Wnt and Fzl gene expression was normalized to 18s rRNA and GAPDH gene expression in the same samples.

FXR, SHP and BSEP mRNA levels were quantified in normal and HCC human cDNA purchased from ORIGENE (Rockville, MD). These cDNA samples have been obtained from a total of 34 HCC and 8 normal livers verified by pathologists prior to

isolation of RNA and conversion to cDNA. The HCC samples included 7 samples of Stage I HCC, 8 samples of Stage II and IIIA of HCC each, and 3 samples of Stage IV HCC (Supplementary Table 1). To study FXR, SHP and BSEP gene expression SYBR Green-based (Applied Biosystems, Carlsbad, CA) Real Time PCR was conducted using the Applied Biosystems Prism 7300 Real-time PCR Instrument as described previously (Thomas et al., 2010). FXR, BSEP and SHP gene expression was normalized to GAPDH gene expression. The primers used in this study are described in Table 1. The specificity of these primers was verified both by agarose gel analysis and by reviewing melting and amplification curves during Real Time PCR.

Statistical Analysis.

Data presented in the form of bar graphs show mean$\pm$SD. To determine statistically significant difference between groups paired Student's T-test was used. Difference between groups was considered statistically significant at $P<0.05$. The different degrees of significance was indicated as follows in the bar graphs- *P<0.5; **P<0.01; ***P<0.001

JPET Fast Forward. Published on March 23, 2011 as DOI: 10.1124/jpet.111.179390
This article has not been copyedited and formatted. The final version may differ from this version.

Results

Extensive hepatic tumor development in FXR-KO mice. We observed extensive hepatic tumors in 100% of 12-14 month old FXR-KO mice whereas none of the age matched WT mice had any tumors. Hematoxylin and Eosin (H&E) staining of paraffin slides indicated normal histology with well-organized hepatic plates radiating from the central vein to the portal areas in the WT mice (Supplementary Fig. 1, upper panel). In FXR-KO mice, the hepatic architecture was severely distorted due to tumor formation. FXR-KO livers had HCC as indicated by the presence of disorganized clear cells, highly eosinophilic cells as well as presence of inflammatory cells in some tumors. PCNA immunohistochemistry indicated less than 0.1% cells in cell cycle in the WT livers (Fig. 1, lower panel) whereas significant proliferation was observed in FXR-KO livers. The rate of proliferation differed in FXR-KO tumors from moderate (Supplementary Fig. 1, lower panel, middle photograph) to very high (Supplementary Fig. 1, lower panel, right photograph) cell proliferation.

Increased β-catenin activation in FXR-KO livers. To determine whether β-catenin activation was observed in the HCC in 12-14 month old FXR-KO livers, we performed Western blot for total and activated β-catenin (dephosphorylated form known to translocate to nucleus). The Western blot analysis indicates moderate increase in total β-catenin protein but a significant increase in activated β-catenin in FXR-KO livers as compared to WT livers (Fig. 1A and B). The ratio of activated to total β-catenin expression indicated 15-fold higher β-catenin activation in the FXR-KO mice (Fig. 1C). Immunohistochemical staining of total β-catenin revealed mainly membranous staining

JPET Fast Forward. Published on March 23, 2011 as DOI: 10.1124/jpet.111.179390
This article has not been copyedited and formatted. The final version may differ from this version.

on hepatocytes in WT mice with no apparent staining for activated β-catenin (Fig. 1D). In contrast, foci of β-catenin positive cells with extensive cytoplasmic stabilization and nuclear translocation of β-catenin were observed in the livers of FXR-KO mice.

Increased β-catenin nuclear localization and target gene expression in FXR-KO livers. We further investigated nuclear localization of β-catenin using immunofluorescence staining method. Immunofluorescence analysis indicated membranous β-catenin staining in WT mice whereas extensive cytoplasmic stabilization and nuclear localization of β-catenin was evident in the FXR-KO livers (Fig. 2A-C). To investigate functional significance of β-catenin activation in FXR-KO livers, we determined levels of β-catenin target gene cyclin D1. Real Time PCR and Western blot analysis (Fig. 2E and D) showed increased mRNA and protein levels of cyclin D1 in FXR-KO livers.

Activation of β-catenin is secondary to GSK-3β inactivation. To identify the mechanism behind β-catenin activation in the FXR-KO mice, we estimated levels of GSK-3β, the main negative regulator of β-catenin in the cells. Western blot analysis (Fig. 3A and B) indicated a moderate decrease in total GSK-3β protein, which was not statistically significant. However, a 3-fold increase in Ser9-phosphorylated (inactive) GSK-3β was observed in FXR-KO livers indicating marked GSK-3β inactivation in FXR-KO mice. In the canonical Wnt signaling pathway an upstream multi-module protein called Dishevelled (Dvl) plays a critical role in regulation of GSK-3β activity. Western

JPET Fast Forward. Published on March 23, 2011 as DOI: 10.1124/jpet.111.179390
This article has not been copyedited and formatted. The final version may differ from this version.

blot analysis of Dvl indicated that FXR-KO livers had a 4-fold increase in total Dvl protein as compared to WT livers. Furthermore, a decrease in Ser45-Thr41-phosphorylated (inactive) β-catenin was observed in FXR-KO liver consistent with increased activation of β-catenin.

Decreased E-cadherin expression in FXR-KO mice. β-Catenin activation is known to be associated with a decrease in E-cadherin expression during carcinogenesis. To study whether loss of E-cadherin may be involved in the pathogenesis of HCC in FXR-KO livers, we estimated levels of E-cadherin in FXR-KO and WT livers. Western blot and immunohistochemical staining (Fig. 4A and C) revealed a substantial decrease in E-cadherin in FXR-KO livers as compared to WT livers. It has been shown that the transcriptional repressor Snail can negatively regulate E-cadherin during tumorigenesis, a process referred to as epithelial-to-mesenchymal transition (EMT). To study whether decreased in E-cadherin levels observed in the FXR-KO livers are associated with increase in Snail, we estimated levels of Snail protein by Western blot. FXR-KO livers had a 2-fold upregulation of Snail as compared to WT livers consistent with decrease in E-cadherin expression (Fig. 4A and B).

Temporal activation of β-catenin in FXR-KO livers. Our data indicate that β-catenin activation is observed in HCC bearing FXR-KO livers at 12-14 months of age. To determine whether β-catenin activation occurs during the tumorigenesis process, we investigated 3 and 8 month old WT and FXR-KO livers. H&E staining revealed no change in WT livers but a moderate dysplasia in the FXR-KO livers (data not shown). β-

JPET Fast Forward. Published on March 23, 2011 as DOI: 10.1124/jpet.111.179390
This article has not been copyedited and formatted. The final version may differ from this version.

Catenin staining and Western blot analysis showed no change in total or activated β-catenin at 3 months of age in the FXR-KO mice as compared to Wt mice (Fig. 5A and B). However, a moderate decrease in total β-catenin and a moderate increase in activated β-catenin were observed in the livers of 8-month-old FXR-KO mice as compared to age matched WT mice (Fig. 5C and D). The ratio of activated to total β-catenin indicated 4-fold higher β-catenin activation in the FXR-KO livers at 8 months of age (Fig. 5F). Immunohistochemical staining revealed numerous foci of hepatocytes with cytoplasmic stabilization and nuclear translocation of β-catenin in 8-month-old FXR-KO livers (Fig. 5E).

Increased Wnt4 and Fzl expression in FXR-KO livers. GSK-3β inactivation and Dvl upregulation in the FXR-KO mice suggests that increased β-catenin activation in the FXR-KO livers could be due to activation of canonical Wnt pathway. The canonical Wnt signaling is initiated by secreted Wnt proteins, which bind to the Frizzled (Fzl) receptors. A total of 19 Wnt and 10 Fzl genes are functional in mammals, out of which 11 Wnts and 8 Fzl genes are expressed in the liver (Zeng et al., 2007). We determined mRNA expression of all 19 Wnts and 10 Fzl genes using TaqMan based Real Time PCR arrays in 8 and 14 month-old WT and FXR-KO livers (Fig. 6). Our analysis indicates that Wnt4 was the only Wnt gene, which was expressed 5-fold higher in the 14-month-old FXR-KO mice (Fig. 6A). Western blot analysis indicated increased Wnt protein expression in the FXR-KO mice at 14 months of age (Fig. 6B). Further we observed induced expression of Fzl1, Fzl4, Fzl7 and Fzl8 mRNA (all 2.5 folds higher) in 14-

month-old FXR-KO livers (Fig. 6C-F). These data indicate that Wnt4 may play a crucial role in stimulation of canonical Wnt signaling in FXR-KO mice.

Decreased FXR expression and activity in human HCC. To investigate whether loss of FXR is relevant to HCC pathogenesis in humans, we investigated FXR gene expression and function in human HCC samples and normal livers by Real Time PCR. The data indicated that FXR expression was decreased to 40% of normal as early as in stage I of HCC (Fig. 7A) and further decreased in stage II, IIIA and IV (20% of normal). To assess change in FXR function, we estimated gene expression of SHP and BSEP, two well-characterized target gene of FXR (Fig. 7B). The data revealed that SHP expression decreased to 20% of normal in stages I to IV of HCC. No difference in BSEP expression was observed in stage I of HCC but BSEP expression decreased to 10% of normal in stages II, IIIA and IV of HCC.

JPET Fast Forward. Published on March 23, 2011 as DOI: 10.1124/jpet.111.179390
This article has not been copyedited and formatted. The final version may differ from this version.

Discussion

HCC is the most common hepatic malignancy with extremely grim prognosis and limited treatment options (El-Serag and Mason, 1999; Befeler and Di Bisceglie, 2002; Di Bisceglie and Befeler, 2007). Whereas the mechanisms of HCC pathogenesis are not completely clear, it has been observed that signaling cross talk between multiple signal transduction pathways are involved in progression of HCC (Aravalli et al., 2008; Llovet and Bruix, 2008). Our studies indicate that signaling cross talk between bile acids, FXR and Wnt/β-catenin pathway may be involved in pathogenesis of HCC.

Previous studies have demonstrated that loss of FXR results in increased tumorigenesis in the colon and the liver (Kim et al., 2007b; Yang et al., 2007; Maran et al., 2009). Whereas two independent groups have observed spontaneous HCC in FXR-KO mice, the mechanisms are not completely clear. We observed spontaneous HCC development in all FXR-KO mice studied at the age of 12 to 14 months corroborating previous findings. Because Wnt/β-catenin signaling has been implicated in pathogenesis of HCC, we investigated whether activation of β-catenin occurs in FXR-KO livers during HCC formation. Our data indicate a significant increase in β-catenin activation in FXR-KO tumors. We also observed a temporal increase in β-catenin activation in the FXR-KO livers during the tumorigenesis process. Kim et al. have previously reported increase in β-catenin mRNA in FXR-KO livers at 3 months but did not observe changes in protein levels, which was attributed to post-transcriptional regulation of β-catenin (Kim et al., 2007b). Consistent with this observation our data indicate no change in β-catenin activation at 3 months of age. However, a significant

JPET Fast Forward. Published on March 23, 2011 as DOI: 10.1124/jpet.111.179390
This article has not been copyedited and formatted. The final version may differ from this version.

increase in β-catenin activation was noted at 8 months of age in FXR-KO livers, which further increased at 14 months. The lack of early increased in β-catenin activation suggests that the mechanisms of β-catenin activation in the FXR-KO mice may be independent of loss of FXR in the FXR-KO mice.

One of the plausible mechanisms behind β-catenin activation is increased bile acids in the FXR-KO mice. FXR-KO mice are known to have 4-fold higher total bile acids but the bile acid composition remains largely unchanged (Kim et al., 2007a; Kim et al., 2007b). However, decreasing bile acids using cholestyramine reduces tumor incidence (Yang et al., 2007). It was also observed that long-term bile acid treatment significantly increased dimethylnitrosamine (DEN)-induced HCC in C57BL/6 mice (Yang et al., 2007). Interestingly, hepatocyte specific FXR knockout mice, which do not have increased bile acids, do not develop HCC (unpublished observations). Further, the bile salt export pump (BSEP) knockout mice, which have increased bile acids, also develop HCC. Furthermore, children with BSEP mutations develop progressive familial intrahepatic cholestasis (PFIC) and are highly susceptible to development of HCC (Knisely et al., 2006). These observations indicate that increased bile acids play a critical role in hepatic tumorigenesis in the FXR-KO mice. Our data suggests the possibility that increased bile acids may stimulate temporal activation of Wnt/β-catenin pathway independent of FXR and promote HCC development in FXR-KO. However, the exact mechanisms by which bile acids induce β-catenin are currently not known. Bile acids are known to initiate FXR-independent signaling via EGFR and ERK-1/2 signaling pathways (Allen et al., 2009; Hylemon et al., 2009). Both ERK-1/2 and AKT signaling pathways are known to interact with Wnt signaling resulting in β-catenin activation (Hu

and Li, 2010). These observations support the hypothesis that increased bile acids in the FXR-KO mice may stimulate β-catenin activation via MAPK signaling.

The molecular mechanism of β-catenin activation in FXR-KO mice seems to be multifold. Our data indicate that both activation of canonical Wnt signaling pathway and loss of E-cadherin are involved in β-catenin activation in FXR-KO livers. Increased Wnt4 and several Fzl receptors, induced Dvl expression, striking inactivation of GSK-3β and decrease in Ser45-Thr41-phosphorylated β-catenin indicate activation of canonical Wnt signaling in FXR-KO livers. However, we cannot exclude the possibility that the inactivation of GSK-3β could be independent of canonical Wnt signaling. Studies have shown that MAPK signaling can cross-activate β-catenin activation via inactivation of GSK-3β (Ding et al., 2005; Hu and Li, 2010). Similarly, it is known that insulin signaling induces GSK-3β inactivation, thus converging insulin signaling and Wnt signaling pathways (Pearl and Barford, 2002). Interestingly, recent evidence suggests that bile acids can activate AKT, EGFR, EKR-1/2 as well as insulin signaling (Hylemon et al., 2009; Trauner et al., 2010). It is plausible that GSK-3β inactivation observed in the FXR-KO mice is due to increased bile acids in these mice. These studies point to the possibility that GSK-3β inactivation observed in FXR-KO mice may be independent of canonical Wnt signaling.

E-cadherin plays an important role in regulation of β-catenin activity in cells by sequestering β-catenin at the cell membrane (Apte et al., 2006; Thompson and Monga, 2007). An increase in β-catenin gene expression results in a concomitant increase in E-

JPET Fast Forward. Published on March 23, 2011 as DOI: 10.1124/jpet.111.179390
This article has not been copyedited and formatted. The final version may differ from this version.

cadherin expression effectively reducing the activity of β-catenin (Apte et al., 2006). Loss of E-cadherin is a hallmark of many cancers resulting in increased cytoplasmic stabilization of β-catenin (Behrens et al., 1993; Nuruki et al., 1998; Calvisi et al., 2004b; Jeanes et al., 2008). We observed a marked decrease in E-cadherin expression in the FXR-KO livers consistent with increased β-catenin activation. A well-known mechanism of inhibited E-cadherin expression is gene repression by transcriptional repressor Snail, which occurs during EMT and is well documented during carcinogenesis (Batlle et al., 2000; Cano et al., 2000; Huber et al., 2005). Further, previous *in vitro* studies indicate that bile acids can induce Snail activation resulting in E-cadherin suppression (Fukase et al., 2008). Consistent with these observations we observed increased in Snail activation in the FXR-KO mice. These data indicate that an EMT-dependent repression of E-cadherin resulting in subsequent β-catenin activation may be involved in the pathogenesis of HCC in FXR-KO mice. The molecular mechanism of decreased E-cadherin expression in the FXR-KO mice is not completely clear. It is possible that increased bile acids in FXR-KO mice induce Snail expression, which suppresses E-cadherin expression. However, recent ChIP-sequencing studies on FXR binding site in liver and intestine indicate that FXR has multiple binding sites upstream of E-cadherin gene in the liver (Thomas et al., 2010). This observation suggests that loss of E-cadherin expression in the FXR-KO mice may be a direct result of FXR deletion. These studies also warrant further analysis of the FXR binding sites on E-cadherin gene.

To examine whether the observation that loss of FXR results in increased HCC development is relevant for human HCC pathogenesis, we studied whether FXR

expression and function decreases in human HCC. Our data indicate decreased FXR mRNA and activity (as demonstrated by decreased SHP expression, a target of FXR) as early as stage I of HCC. Whereas these data do not provide an evidence for FXR loss during HCC pathogenesis, they do indicate that loss of FXR function is associated with HCC and thus may be involved in HCC development. Detailed analysis of FXR expression, function and bile acid levels during various stages of HCC pathogenesis including steatohepatitis, fibrosis, and cirrhosis is required for further understanding the role of FXR and bile acids in pathogenesis of HCC, which are beyond the scope of this manuscript.

Taken together, these data provide strong evidence for increased Wnt/β-catenin pathway activation during HCC development in FXR-KO mice. These observations also provide basis for the hypothesis that increased bile acids promote HCC development via stimulation of Wnt signaling. Whereas further studies using tissue specific double knockout mice and modulation of total bile acid levels are required to test this hypothesis, the present observations support a role for β-catenin activation during pathogenesis of HCC in the FXR-KO mice. These data indicate that a detailed analysis of FXR, bile acids and Wnt signaling will reveal novel therapeutic targets for HCC treatment.

Acknowledgements

The authors would like to thank Guodong Li and Marimaran Rengasamy for technical support.

Authorship Contributions

Participated in research design: Udayan Apte, Grace Guo, Andy Wolfe

Conducted Research: Andy Wolfe, Reshma Jaseja, Ann Thomas, Genea Edwards

Data Analysis: Udayan Apte, Andy Wolfe, Grace Guo, Ann Thomas

Wrote the manuscript: Udayan Apte, Grace Guo

References

Allen K, Kim ND, Moon JO and Copple BL (2009) Upregulation of early growth response factor-1 by bile acids requires mitogen-activated protein kinase signaling. *Toxicol Appl Pharmacol*.

Apte U, Singh S, Zeng G, Cieply B, Virji MA, Wu T and Monga SP (2009) Beta-catenin activation promotes liver regeneration after acetaminophen-induced injury. *Am J Pathol* **175**:1056-1065.

Apte U, Zeng G, Muller P, Tan X, Micsenyi A, Cieply B, Dai C, Liu Y, Kaestner KH and Monga SP (2006) Activation of Wnt/beta-catenin pathway during hepatocyte growth factor-induced hepatomegaly in mice. *Hepatology* **44**:992-1002.

Aravalli RN, Steer CJ and Cressman EN (2008) Molecular mechanisms of hepatocellular carcinoma. *Hepatology* **48**:2047-2063.

Batlle E, Sancho E, Franci C, Dominguez D, Monfar M, Baulida J and Garcia De Herreros A (2000) The transcription factor snail is a repressor of E-cadherin gene expression in epithelial tumour cells. *Nat Cell Biol* **2**:84-89.

Befeler AS and Di Bisceglie AM (2002) Hepatocellular carcinoma: diagnosis and treatment. *Gastroenterology* **122**:1609-1619.

Behrens J, Vakaet L, Friis R, Winterhager E, Van Roy F, Mareel MM and Birchmeier W (1993) Loss of epithelial differentiation and gain of invasiveness correlates with tyrosine phosphorylation of the E-cadherin/beta-catenin complex in cells transformed with a temperature-sensitive v-SRC gene. *J Cell Biol* **120**:757-766.

Calvisi DF, Factor VM, Ladu S, Conner EA and Thorgeirsson SS (2004a) Disruption of beta-catenin pathway or genomic instability define two distinct categories of liver cancer in transgenic mice. *Gastroenterology* **126**:1374-1386.

Calvisi DF, Ladu S, Conner EA, Factor VM and Thorgeirsson SS (2004b) Disregulation of E-cadherin in transgenic mouse models of liver cancer. *Lab Invest* **84**:1137-1147.

Cano A, Perez-Moreno MA, Rodrigo I, Locascio A, Blanco MJ, del Barrio MG, Portillo F and Nieto MA (2000) The transcription factor snail controls epithelial-mesenchymal transitions by repressing E-cadherin expression. *Nat Cell Biol* **2**:76-83.

Carruba G, Cervello M, Miceli MD, Farruggio R, Notarbartolo M, Virruso L, Giannitrapani L, Gambino R, Montalto G and Castagnetta L (1999) Truncated form of beta-catenin and reduced expression of wild-type catenins feature HepG2 human liver cancer cells. *Ann N Y Acad Sci* **886**:212-216.

Devereux TR, Stern MC, Flake GP, Yu MC, Zhang ZQ, London SJ and Taylor JA (2001) CTNNB1 mutations and beta-catenin protein accumulation in human hepatocellular carcinomas associated with high exposure to aflatoxin B1. *Mol Carcinog* **31**:68-73.

Di Bisceglie AM and Befeler AS (2007) Diagnostic and therapeutic approach to hepatocellular carcinoma in the USA. *Hepatol Res* **37 Suppl 2**:S251-253.

Ding Q, Xia W, Liu JC, Yang JY, Lee DF, Xia J, Bartholomeusz G, Li Y, Pan Y, Li Z, Bargou RC, Qin J, Lai CC, Tsai FJ, Tsai CH and Hung MC (2005) Erk associates with and primes GSK-3beta for its inactivation resulting in upregulation of beta-catenin. *Mol Cell* **19**:159-170.

El-Serag HB and Mason AC (1999) Rising incidence of hepatocellular carcinoma in the United States. *N Engl J Med* **340**:745-750.

Eloranta JJ and Kullak-Ublick GA (2008) The role of FXR in disorders of bile acid homeostasis. *Physiology (Bethesda)* **23**:286-295.

Forman BM, Goode E, Chen J, Oro AE, Bradley DJ, Perlmann T, Noonan DJ, Burka LT, McMorris T, Lamph WW, Evans RM and Weinberger C (1995) Identification of a nuclear receptor that is activated by farnesol metabolites. *Cell* **81**:687-693.

Fujie H, Moriya K, Shintani Y, Tsutsumi T, Takayama T, Makuuchi M, Kimura S and Koike K (2001) Frequent beta-catenin aberration in human hepatocellular carcinoma. *Hepatol Res* **20**:39-51.

Fukase K, Ohtsuka H, Onogawa T, Oshio H, Ii T, Mutoh M, Katayose Y, Rikiyama T, Oikawa M, Motoi F, Egawa S, Abe T and Unno M (2008) Bile acids repress E-cadherin through the induction of Snail and increase cancer invasiveness in human hepatobiliary carcinoma. *Cancer Sci* **99**:1785-1792.

Gadaleta RM, van Mil SW, Oldenburg B, Siersema PD, Klomp LW and van Erpecum KJ (2010) Bile acids and their nuclear receptor FXR: Relevance for hepatobiliary and gastrointestinal disease. *Biochim Biophys Acta* **1801**:683-692.

Guo GL, Lambert G, Negishi M, Ward JM, Brewer HB, Jr., Kliewer SA, Gonzalez FJ and Sinal CJ (2003) Complementary roles of farnesoid X receptor, pregnane X receptor, and constitutive androstane receptor in protection against bile acid toxicity. *J Biol Chem* **278**:45062-45071.

Hu T and Li C (2010) Convergence between Wnt-beta-catenin and EGFR signaling in cancer. *Mol Cancer* **9**:236.

Huang H, Fujii H, Sankila A, Mahler-Araujo BM, Matsuda M, Cathomas G and Ohgaki H (1999) Beta-catenin mutations are frequent in human hepatocellular carcinomas associated with hepatitis C virus infection. *Am J Pathol* **155**:1795-1801.

Huang W, Ma K, Zhang J, Qatanani M, Cuvillier J, Liu J, Dong B, Huang X and Moore DD (2006) Nuclear receptor-dependent bile acid signaling is required for normal liver regeneration. *Science* **312**:233-236.

Huber MA, Kraut N and Beug H (2005) Molecular requirements for epithelial-mesenchymal transition during tumor progression. *Curr Opin Cell Biol* **17**:548-558.

Hylemon PB, Zhou H, Pandak WM, Ren S, Gil G and Dent P (2009) Bile acids as regulatory molecules. *J Lipid Res* **50**:1509-1520.

Jeanes A, Gottardi CJ and Yap AS (2008) Cadherins and cancer: how does cadherin dysfunction promote tumor progression? *Oncogene* **27**:6920-6929.

Kim I, Ahn SH, Inagaki T, Choi M, Ito S, Guo GL, Kliewer SA and Gonzalez FJ (2007a) Differential regulation of bile acid homeostasis by the farnesoid X receptor in liver and intestine. *J Lipid Res* **48**:2664-2672.

Kim I, Morimura K, Shah Y, Yang Q, Ward JM and Gonzalez FJ (2007b) Spontaneous hepatocarcinogenesis in farnesoid X receptor-null mice. *Carcinogenesis* **28**:940-946.

Knisely AS, Strautnieks SS, Meier Y, Stieger B, Byrne JA, Portmann BC, Bull LN, Pawlikowska L, Bilezikci B, Ozcay F, Laszlo A, Tiszlavicz L, Moore L, Raftos J, Arnell H, Fischler B, Nemeth A, Papadogiannakis N, Cielecka-Kuszyk J, Jankowska I, Pawlowska J, Melin-Aldana H, Emerick KM, Whitington PF, Mieli-Vergani G and Thompson RJ (2006) Hepatocellular carcinoma in ten children under five years of age with bile salt export pump deficiency. *Hepatology* **44**:478-486.

Kolligs FT, Bommer G and Goke B (2002) Wnt/beta-catenin/tcf signaling: a critical pathway in gastrointestinal tumorigenesis. *Digestion* **66**:131-144.

Lambert G, Amar MJ, Guo G, Brewer HB, Jr., Gonzalez FJ and Sinal CJ (2003) The farnesoid X-receptor is an essential regulator of cholesterol homeostasis. *J Biol Chem* **278**:2563-2570.
Llovet JM and Bruix J (2008) Molecular targeted therapies in hepatocellular carcinoma. *Hepatology* **48**:1312-1327.

Maran RR, Thomas A, Roth M, Sheng Z, Esterly N, Pinson D, Gao X, Zhang Y, Ganapathy V, Gonzalez FJ and Guo GL (2009) Farnesoid X receptor deficiency in mice leads to increased intestinal epithelial cell proliferation and tumor development. *J Pharmacol Exp Ther* **328**:469-477.

Modica S, Murzilli S, Salvatore L, Schmidt DR and Moschetta A (2008) Nuclear bile acid receptor FXR protects against intestinal tumorigenesis. *Cancer Res* **68**:9589-9594.

Monga SP, Micsenyi A, Germinaro M, Apte U and Bell A (2006) beta-Catenin regulation during matrigel-induced rat hepatocyte differentiation. *Cell Tissue Res* **323**:71-79.

Monga SP, Monga HK, Tan X, Mule K, Pediaditakis P and Michalopoulos GK (2003) Beta-catenin antisense studies in embryonic liver cultures: role in proliferation, apoptosis, and lineage specification. *Gastroenterology* **124**:202-216.

Nuruki K, Toyoyama H, Ueno S, Hamanoue M, Tanabe G, Aikou T and Ozawa M (1998) E-cadherin but not N-cadherin expression is correlated with the intracellular distribution of catenins in human hepatocellular carcinomas. *Oncol Rep* **5**:1109-1114.

Pearl LH and Barford D (2002) Regulation of protein kinases in insulin, growth factor and Wnt signalling. *Curr Opin Struct Biol* **12**:761-767.

Sinal CJ, Tohkin M, Miyata M, Ward JM, Lambert G and Gonzalez FJ (2000) Targeted disruption of the nuclear receptor FXR/BAR impairs bile acid and lipid homeostasis. *Cell* **102**:731-744.

Taniguchi K, Roberts LR, Aderca IN, Dong X, Qian C, Murphy LM, Nagorney DM, Burgart LJ, Roche PC, Smith DI, Ross JA and Liu W (2002) Mutational spectrum of beta-catenin, AXIN1, and AXIN2 in hepatocellular carcinomas and hepatoblastomas. *Oncogene* **21**:4863-4871.

Thomas AM, Hart SN, Kong B, Fang J, Zhong XB and Guo GL (2010) Genome-wide tissue-specific farnesoid X receptor binding in mouse liver and intestine. *Hepatology* **51**:1410-1419.

Thompson MD and Monga SP (2007) WNT/beta-catenin signaling in liver health and disease. *Hepatology* **45**:1298-1305.

Trauner M, Claudel T, Fickert P, Moustafa T and Wagner M (2010) Bile acids as regulators of hepatic lipid and glucose metabolism. *Dig Dis* **28**:220-224.

Wang YD, Chen WD, Moore DD and Huang W (2008) FXR: a metabolic regulator and cell protector. *Cell Res* **18**:1087-1095.

Yang F, Huang X, Yi T, Yen Y, Moore DD and Huang W (2007) Spontaneous development of liver tumors in the absence of the bile acid receptor farnesoid X receptor. *Cancer Res* **67**:863-867.

Zeng G, Awan F, Otruba W, Muller P, Apte U, Tan X, Gandhi C, Demetris AJ and Monga SP (2007) Wnt'er in liver: expression of Wnt and frizzled genes in mouse. *Hepatology* **45**:195-204.

Footnotes:

This works was supported by National Institutes of Health National Center for Research Resources (NIH 1 P20 RR021940-03); National Institutes of Health National Institute of Diabetes and Digestive and Kidney Diseases (R01 DK031343); and University of Kansas Endowment Startup Funds.

JPET Fast Forward. Published on March 23, 2011 as DOI: 10.1124/jpet.111.179390
This article has not been copyedited and formatted. The final version may differ from this version.

Figure Legends

Figure 1. Increased activation of β-catenin in the livers of FXR-KO mice. **A:** Western blot analysis for total and activated (dephosphorylated) β-catenin using WT and FXR-KO total liver extracts **B:** Densitometric analysis of total and activated β-catenin Western blots from WT and FXR-KO liver homogenates in "A". Data are expressed as mean±SD. Statistical significance: * *p< 0.05* **C:** Bar graph showing ratio of activated to total β-catenin in the livers of WT and FXR-KO mice. **D:** Representative photomicrographs of total β-catenin immunohistochemistry on WT and FXR-KO livers. Representative photographs of 2 WT and 4 independent FXR-KO livers have been shown. Arrowheads point to cytoplasmic and nuclear stabilization of β-catenin. Magnification 400x.

Figure 2. β-Catenin activation results in cyclin D1 upregulation and is regulated by canonical signaling in FXR-KO mice. **A-C**: Immunofluorescence staining of total β-catenin in WT (A) and FXR-KO mice (B, 400x; C, 600x). Arrowheads point to cytoplasmic and nuclear stabilization of β-catenin. Western blot analysis of cyclin D1 using WT and FXR-KO total liver homogenates. **D:** Real Time PCR analysis of cyclin D1 in WT and FXR-KO livers. Data are expressed as mean±SD. Statistical significance: * *p< 0.05*.

Figure 3. Increased GSK-3β inactivation in FXR-KO mice. **A:** Western blot analysis of total and Ser9-phosphorylated GSK-3β, Ser45-Thr41-phosphorylated β-catenin and

dishevelled (Dvl) performed using WT and FXR-KO liver homogenates. **B:** Densitometric analysis of blots in "A". Data are expressed as mean±SD. Statistical significance: * *p< 0.05*, ** *P<0.01*

Figure 4. Loss of E-cadherin as a mechanism of β-catenin activation. **A:** Western blots of E-cadherin and Snail conducted using WT and FXR-KO liver homogenates. **B:** Densitometric analysis of E-cadherin and Snail Western blots. Western blots from 3 separate mice were scanned and used for densitometric analysis in "A". Data are expressed as mean±SD. Statistical significance: * *p< 0.05, ** P<0.01, ***P<0.001* **C:** Representative photographs of E-cadherin immunohistochemistry on paraffin sections of WT and FXR-KO. Arrowheads indicate E-cadherin staining on cell membranes.

Figure 5. Temporal increase in β-catenin activation in the livers of FXR-KO mice. **A:** Western blot analysis of total and activated β-catenin in 3-month-old WT and FXR-KO livers. **B:** Representative photomicrographs of β-catenin immunohistochemistry in 3-month-old WT and FXR-KO livers. Arrows indicate membranous β-catenin staining. **C:** Western blot analysis of total and activated β-catenin in 8-month-old WT and FXR-KO livers. **D:** Densitometry of blots in 'D'. Data are expressed as mean±SD. Statistical significance: * *p< 0.05*, ** *P<0.01, ***P<0.001* **E:** Representative photomicrographs of immunohistochemical staining for total β-catenin (i) and activated β-catenin (ii) in WT mice and total β-catenin (iii) and activated β-catenin (iv) in FXR-KO mice. (v) Shows high magnification (600x) photomicrograph of activated β-catenin immunohistochemistry

in FXR-KO livers at 8 months of age. **F:** Bar graph showing ratio of activated to total β-catenin in the livers of 8-month-old WT and FXR-KO mice.

Figure 6. Increased Wnt and Fzl expression in FXR-KO mice. (A) Real Time PCR analysis of Wnt4 in 8 and 14 month old WT and FXR-KO livers. (B) Western blot analysis and densitometric analysis of the Western blots for Wnt4 in 14 month old WT and FXR-KO mice livers. Real Time PCR analysis of (C) Fzl1, (D)Fzl4, (E)Fzl7, (E) Fzl8 in 8 and 14 month old WT and FXR-KO mice. Data are expressed as mean±SD. Statistical significance: * *p< 0.05*, ** *P<0.01, ***P<0.001*.

Figure 7. Decreased FXR expression and activity in human HCC. Total of 40 HCC and 8 normal liver samples were studied. **A:** FXR and **B:** SHP and **C:** BSEP mRNA expression detected by Real Time PCR using normal liver samples and liver samples of various stages of HCC. Data are expressed as mean±SD. Statistical significance: * *p< 0.05*, ** *P<0.01, ***P<0.001*. All comparisons are between the normal livers and the respective stage of HCC.

JPET Fast Forward. Published on March 23, 2011 as DOI: 10.1124/jpet.111.179390
This article has not been copyedited and formatted. The final version may differ from this version.

Table 1. Primers used for Real Time PCR Analysis

Gene Symbol	5' Primer Sequence	3' Primer Sequence
hGAPDH	5’-GGTGGTCTCCTCTGACTTCAA-3’	5’-GTTGCTGTAGCCAAATTCGTTGT-3’
hFXR	5'-TGCATTGAAGTTGCTCTCAGGT-3'	5'-CGCCTGACTGAATTACGGACA-3'
hBSEP	5'-AGTTGCTCATCGCTTGTCTACG-3'	5'-GCTTGATTTCCCTGGCTTTG-3'
hSHP	5’-AGCTGGAAGTGAGAGCAGATCC-3’	5’-AGAAGTGCGTAGAGAATGGCG-3’

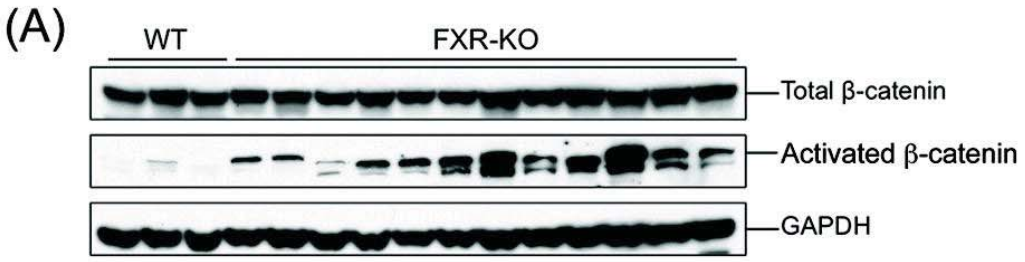

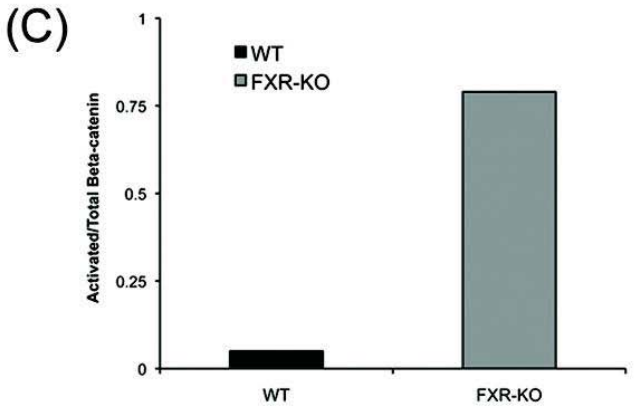

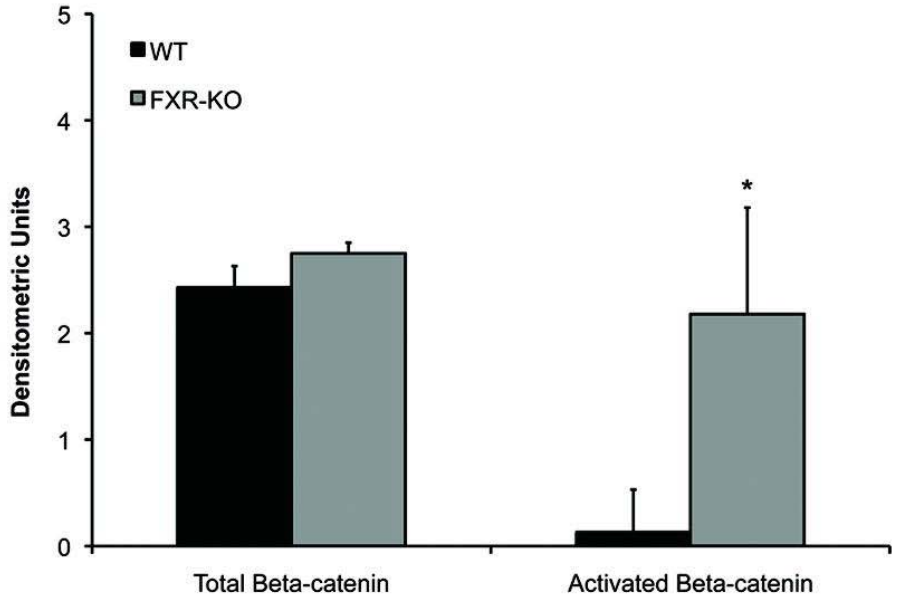

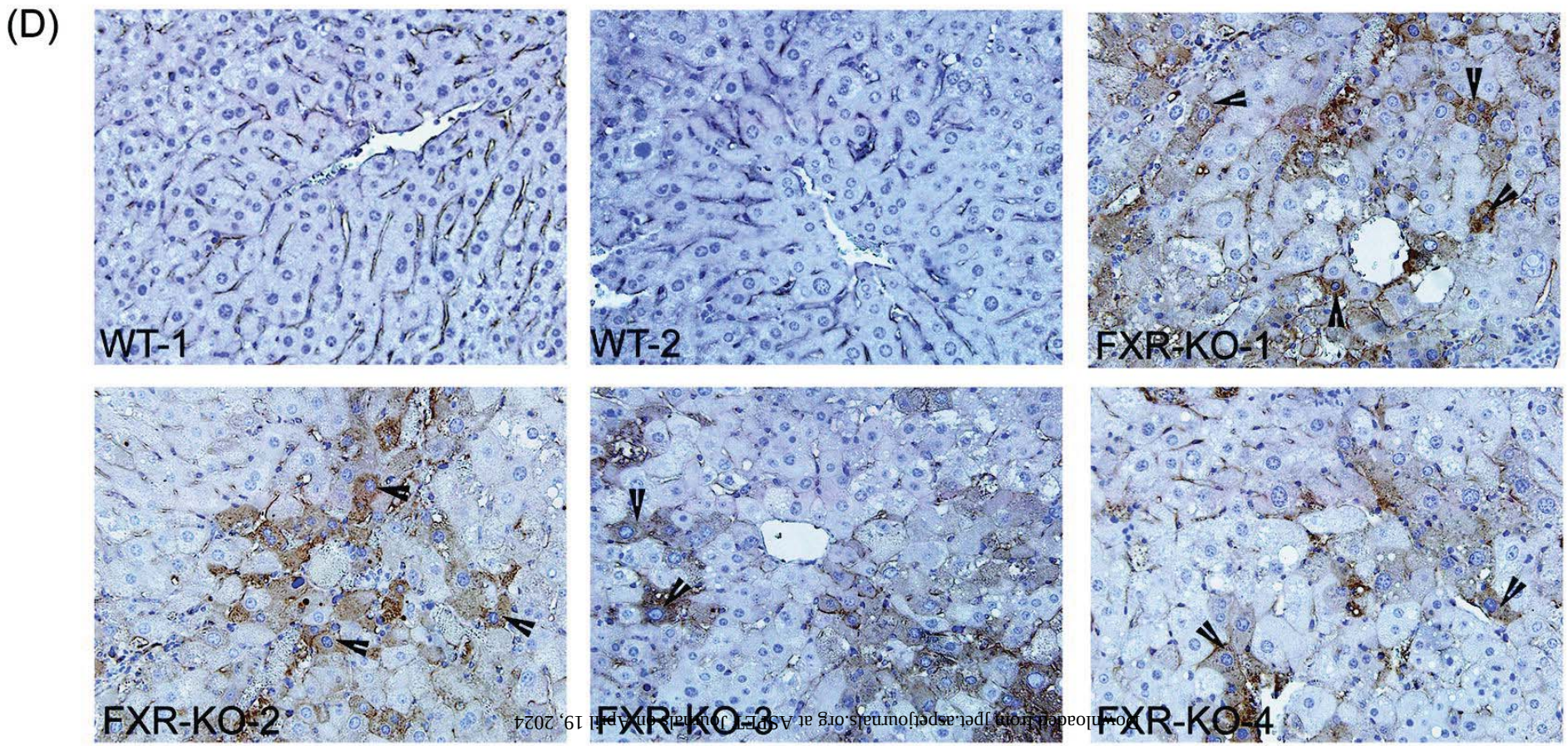

Figure 2

Figure 3

Figure 4

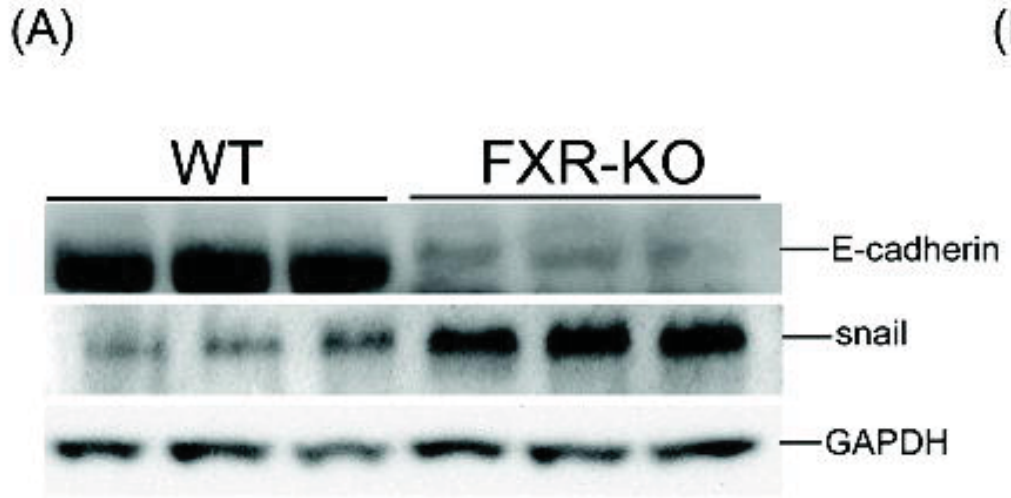

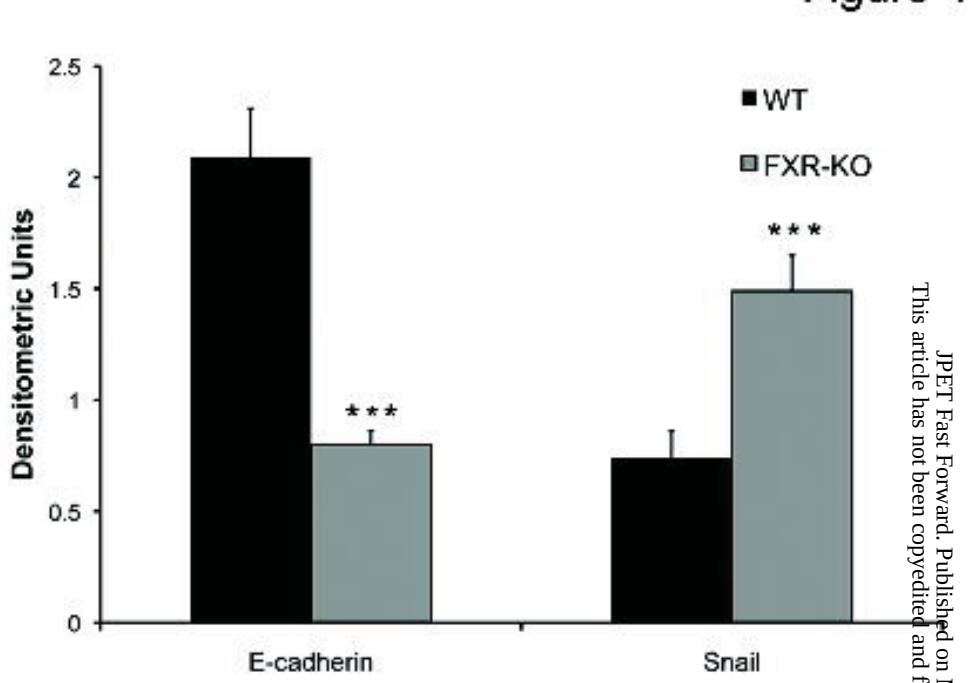

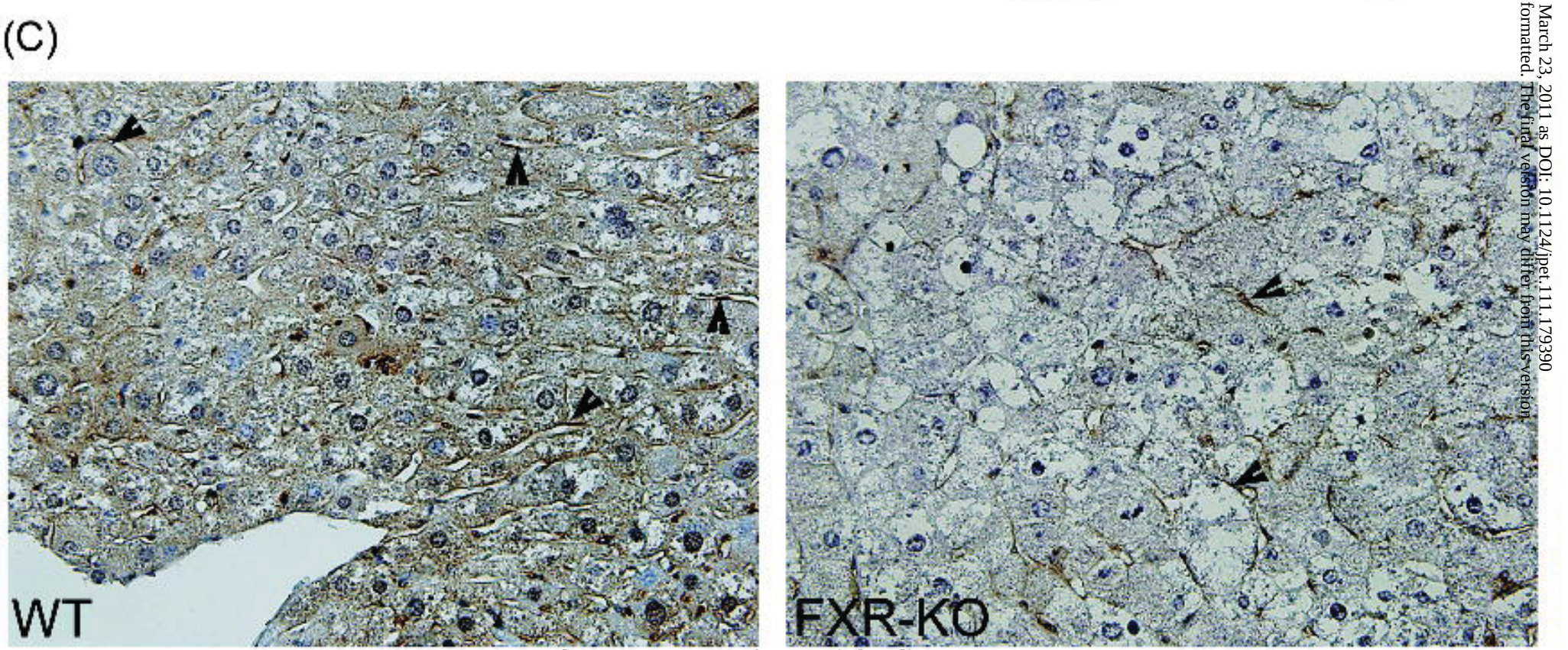

Figure 5

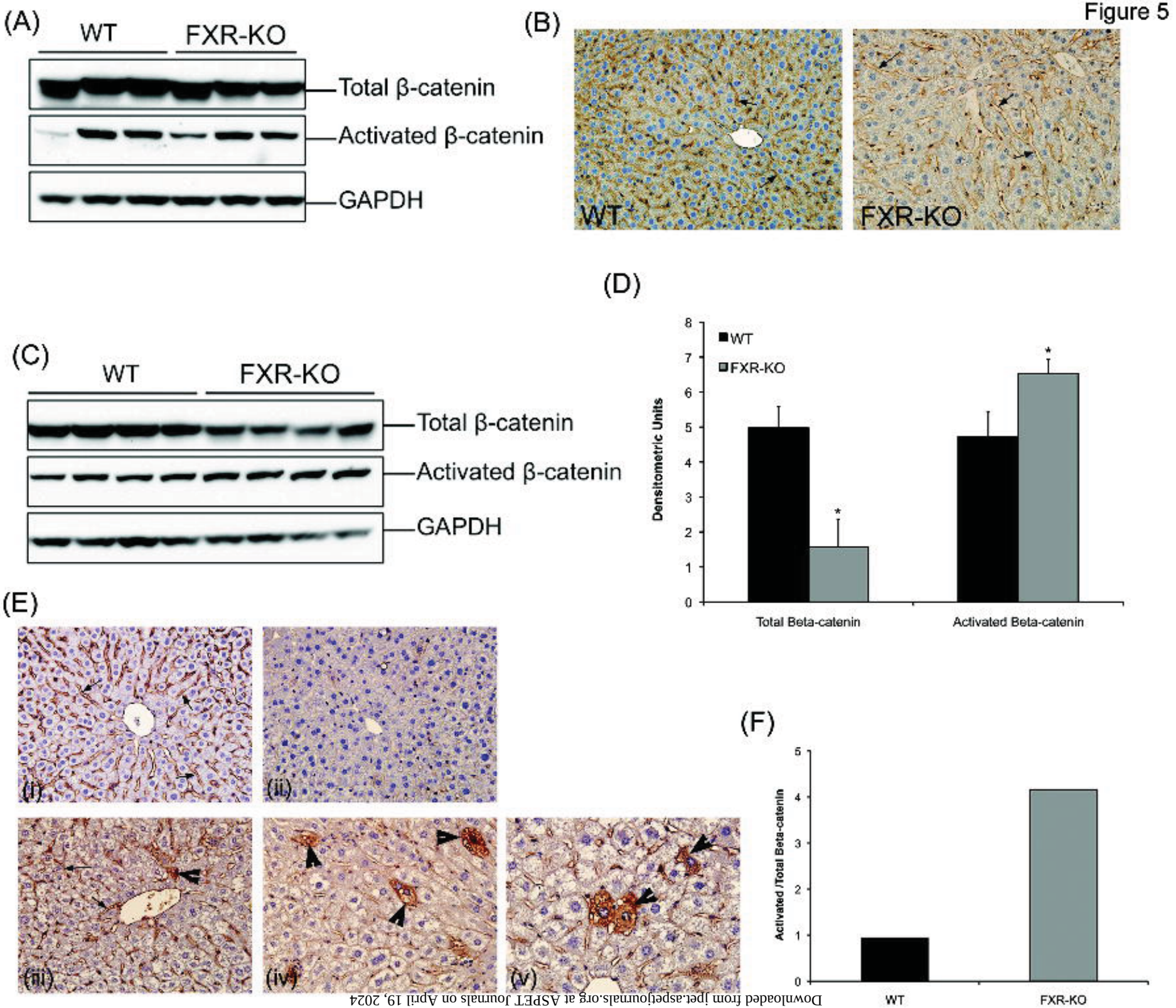

JPET Fast Forward. Published on March 23, 2011 as DOI: 10.1124/jpet.111.179390
This article has not been copyedited and formatted. The final version may differ from this version.

Figure 6

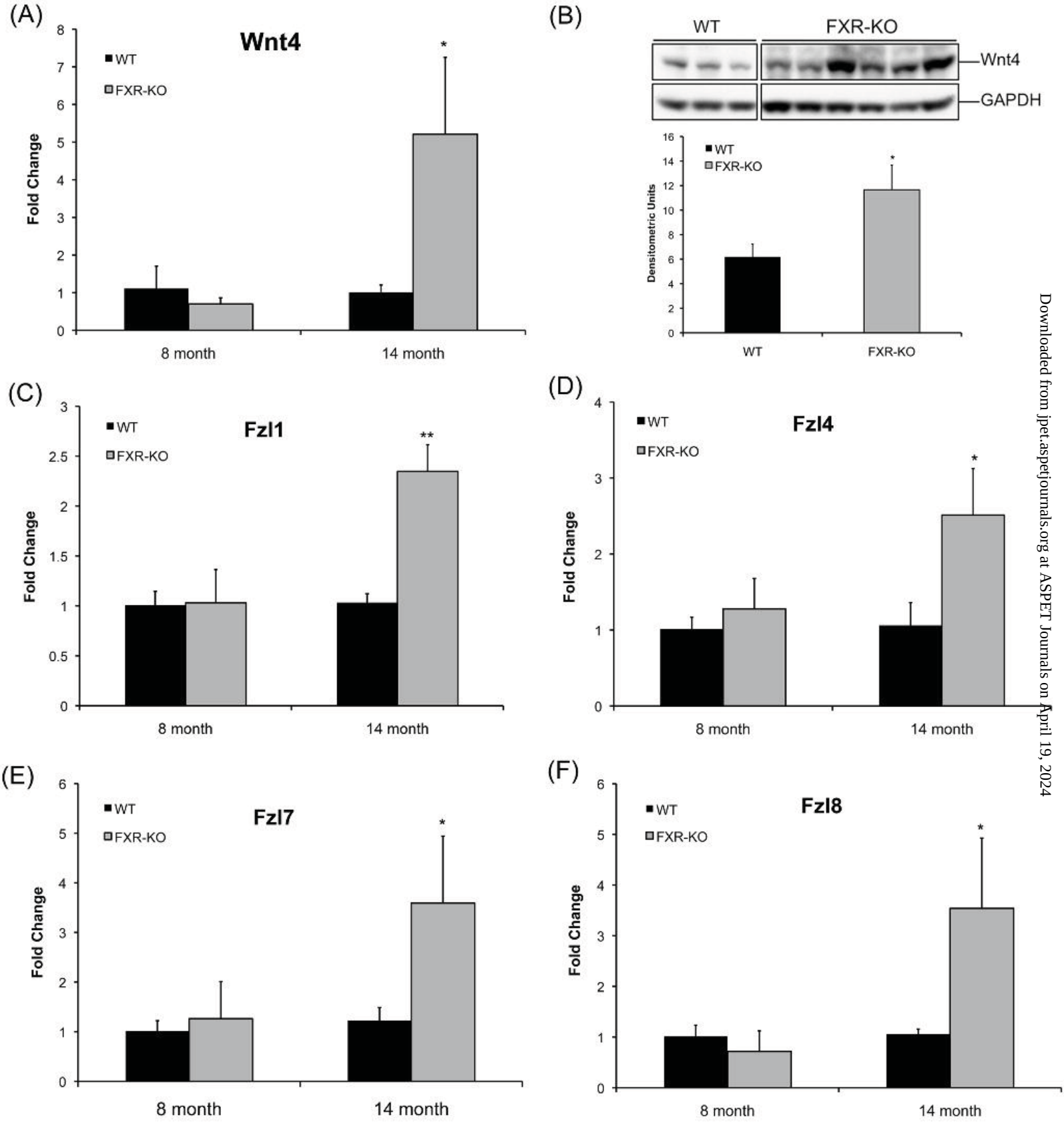

JPET Fast Forward. Published on March 23, 2011 as DOI: 10.1124/jpet.111.179390

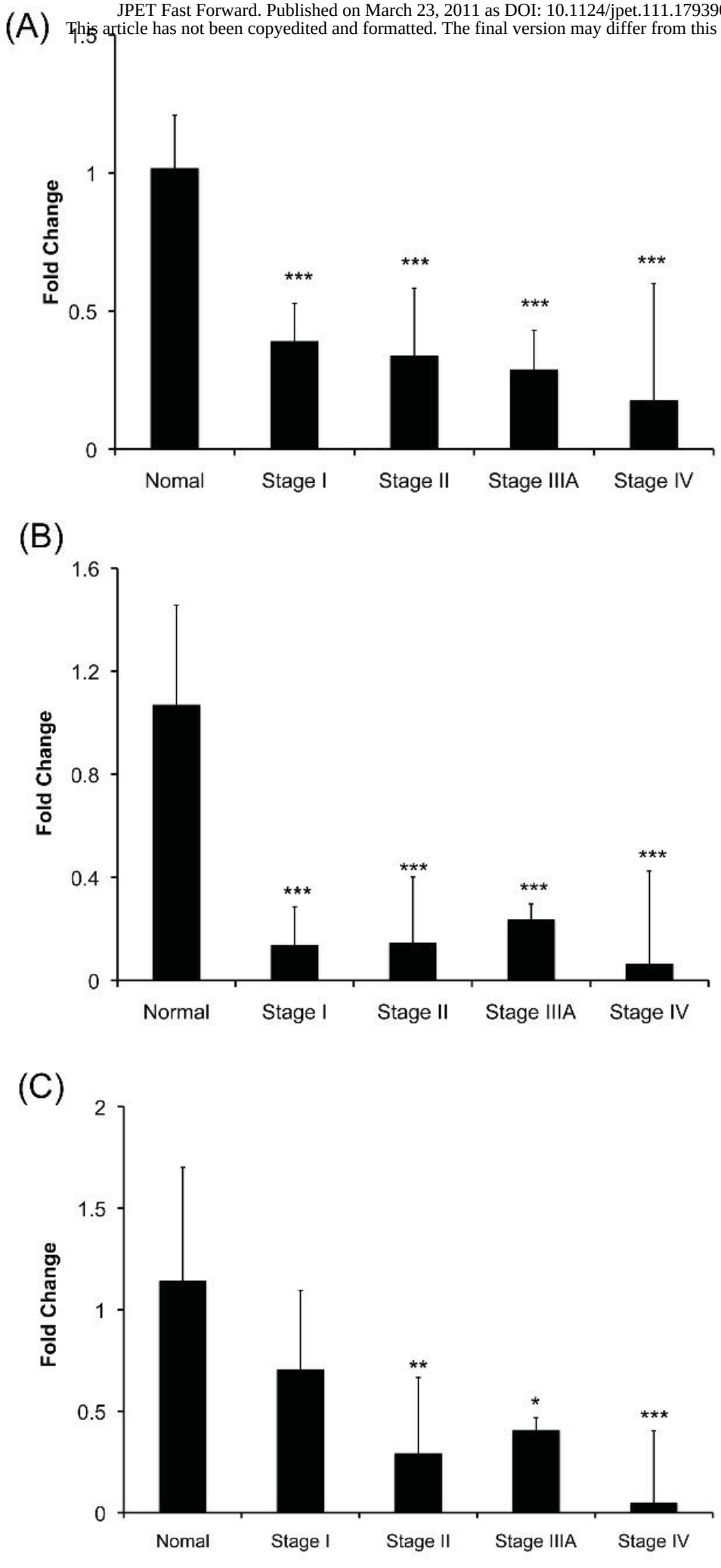

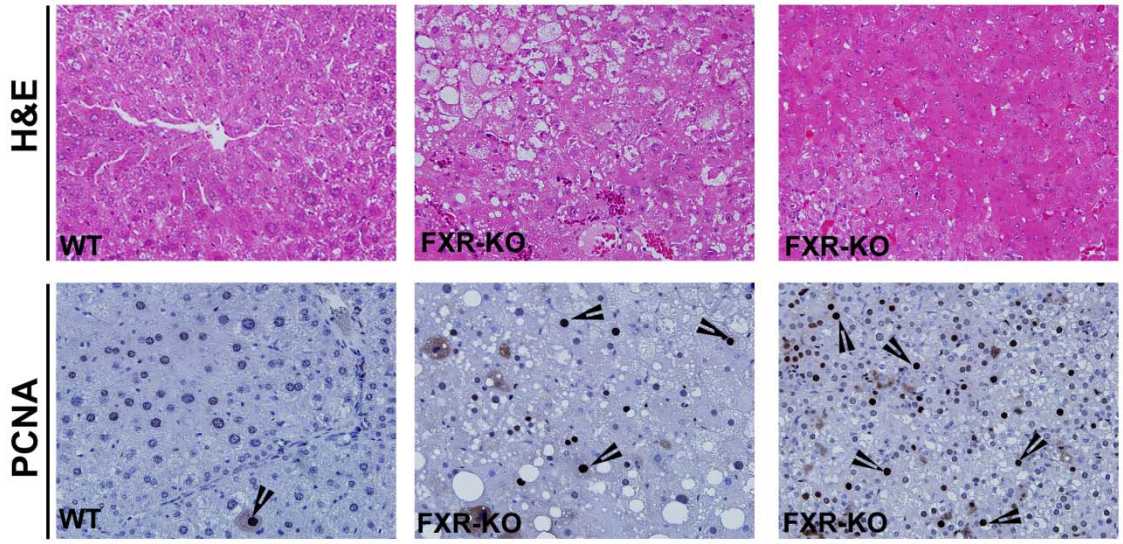

Supplementary Figure 1. Pathological characteristics of spontaneous HCC in FXR-KO mice. *Upper panel,* Representative photographs of H&E stained paraffin sections of livers from WT and FXR-KO mice. *Lower panel*, Representative photographs of the PCNA immunohistochemistry on liver sections from WT and FXR-KO livers. Arrowheads point to cells in S-phase of cell cycle. Magnification 400x.

Increased Activation of Wnt/β-catenin Pathway in Spontaneous Hepatocellular Carcinoma observed in Farnesoid X Receptor Knockout Mice. Wolfe A, Thomas A, Edwards G, Jaseja R, Guo GL, and Apte U. **Journal of Pharmacology and Experimental Therapeutics**

Supplementary Table 1. Clinical Characteristics of normal and HCC samples used in the study.

Gender	Age	Diagnosis	Tumor Grade	Stage
Male	81	Normal	N/A	N/A
Male	73	Normal	N/A	N/A
Male	71	Normal	N/A	N/A
Male	86	Normal	N/A	N/A
Male	52	Normal	N/A	N/A
Female	33	Normal	N/A	N/A
Male	66	Normal	N/A	N/A
Male	68	Normal	N/A	N/A
Male	81	Hepatocellular Carcinoma	AJCC G1: Well differentiated	I
Male	79	Hepatocellular Carcinoma	AJCC G2: Moderately differentiated	I
Female	61	Hepatocellular Carcinoma	AJCC G1: Well differentiated	I
Female	58	Hepatocellular Carcinoma	Unknown	I
Male	66	Hepatocellular Carcinoma	AJCC G3: Poorly differentiated	I
Female	62	Cholangiocarcinoma	AJCC G2: Moderately differentiated	I
Female	78	Cholangiocarcinoma	AJCC G2: Moderately differentiated	I
Female	63	Hepatocellular Carcinoma	AJCC G2: Moderately differentiated	II

Male	73	Hepatocellular Carcinoma	AJCC G2: Moderately differentiated	II
Male	68	Hepatocellular Carcinoma	Not Reported	II
Male	60	Hepatocellular Carcinoma	AJCC G3: Poorly differentiated	II
Female	62	Hepatocellular Carcinoma	AJCC G1: Well differentiated	II
Male	60	Hepatocellular Carcinoma	AJCC G2: Moderately differentiated	II
Male	77	Hepatocellular Carcinoma	AJCC G1: Well differentiated	II
Male	63	Hepatocellular Carcinoma	AJCC G2: Moderately differentiated	II
Female	39	Hepatocellular Carcinoma	AJCC G1: Well differentiated	IIIA
Male	43	Hepatocellular Carcinoma	AJCC G3: Poorly differentiated	IIIA
Female	79	Hepatocellular Carcinoma	AJCC G2: Moderately differentiated	IIIA
Male	56	Hepatocellular Carcinoma	AJCC G2: Moderately differentiated	IIIA
Male	71	Hepatocellular Carcinoma	AJCC G2: Moderately differentiated	IIIA
Male	86	Hepatocellular Carcinoma	AJCC G1: Well differentiated	IIIA
Male	26	Hepatocellular Carcinoma	AJCC G2: Moderately differentiated	IIIA
Male	68	Hepatocellular Carcinoma	AJCC G2: Moderately differentiated	IIIA

Increased Activation of Wnt/β-catenin Pathway in Spontaneous Hepatocellular Carcinoma observed in Farnesoid X Receptor Knockout Mice. Wolfe A, Thomas A, Edwards G, Jaseja R, Guo GL, and Apte U. **Journal of Pharmacology and Experimental Therapeutics**

Male	21	Hepatocellular Carcinoma	AJCC G2: Moderately differentiated	IV
Male	70	Hepatocellular Carcinoma, metastatic	AJCC G3: Poorly differentiated	IV
Male	66	Cholangiocarcinoma of liver, metastatic	Unknown	IV